

# Study on the morphology and tribological properties of acrylic based polyurethane/fumed silica composite coatings

SHUXUE ZHOU

*Department of Materials Science, The Advanced Coatings Research Center of China Educational Ministry, Fudan University, Shanghai 200433, People's Republic of China*

LIMIN WU\*

*Department of Materials Science, The Advanced Coatings Research Center of China Educational Ministry, Fudan University, Shanghai 200433, People's Republic of China; College of Chemistry and Materials Science, Hubei University, Wuhan 430062, People's Republic of China  
E-mail: lxw@fudan.ac.cn*

WEIDIAN SHEN

*Department of Physics and Astronomy, Eastern Michigan University, Ypsilanti, MI 48197, USA*

GUANGXIN GU

*Department of Materials Science, The Advanced Coatings Research Center of China Educational Ministry, Fudan University, Shanghai 200433, People's Republic of China*

Two fumed silica (one hydrophilic and one hydrophobic) were used in the high solid acrylic based polyurethane coatings by directly mixing. The dispersion of fumed silica particles in the bulk of polyurethane coats was characterized by transmission electron microscope (TEM) and surface morphology examined using a scanning probe microscope (SPM). Micro indentation and scratching tests were carried out with a nano-indenter. Both hydrophilic and hydrophobic fumed silica nearly have the same dispersion in acrylic based polyurethane coats. The surface roughness of polyurethane coats increases as fumed silica increases, however, the surfaces of polyurethane coatings containing hydrophobic fumed silica are rougher than that containing hydrophilic fumed silica at the same content. Addition of fumed silica can obviously enhance the micro indentation hardness (MIH) and elastic modulus of polyurethane coats and the higher the content of fumed silica is, the higher the MIH is for hydrophilic one but for hydrophobic one only under normal load less than 20 mN. In the micro scratch experiment, the elastic response and plastic deformation nearly keep constant with normal force increasing for pure acrylic based polyurethane coats. But the percentage of elastic response decreases and the percentage of plastic deformation increases as normal force increases for the polyurethane coats with fumed silica. Crack occurs when scratching under normal force higher than 50 mN for the polyurethane coats with fumed silica, and as the content of fumed silica increases, the critical force for crack increases. Additionally, both hydrophilic and hydrophobic fumed silica have no obvious influence on the response to mar stress and micro mar resistance (MMR) of acrylic based polyurethane. © 2004 Kluwer Academic Publishers

## 1. Introduction

Fumed silica has been successfully used as the rheological additive for adhesives, resins, and paints [1, 2]. Especially, its effects on the rheological behavior of different coatings are extensively investigated and reported [3–5]. However, besides as rheological additive, fumed silica can also be regarded as filler in polymers to

improve their mechanical properties [5, 6]. Since fumed silica has its primary particle size in nanoscale (usually in the range of 10–20 nm), it can be used as the nanoparticles in the preparation of organic-inorganic nanocomposites. For example, Ou *et al.* [7] adopted fumed silica to prepare poly(methyl methacrylate) (PMMA)/silica nanocomposites. In the U.S. Patent [8], nano-SiO<sub>2</sub>

\* Author to whom all correspondence should be addressed.

particles, actually fumed silica, were used to improve scratch resistance of a coating while keep the coating clear appearance.

Acrylic polyol resin cured with polyisocyanate or melamine is widely used in automotive coatings, furniture coatings, machine coatings and etc. to improve the performance of coatings. However, acrylic based coatings, expected to possess better mechanical properties, such as hardness, scratch resistance and abrasion resistance, are more desirable. Here, fumed silica is expected to improve the hardness or scratch resistance of high solid acrylic based polyurethane coatings. Scratch resistance can be characterized by the gloss retention after scraping with rotating brush [9]. In recent years, a new approach to characterize scratch and mar resistance of coatings was developed using a modified scanning probe microscope and a nano-indenter [10–13]. In this paper, micro indentation and scratching tests were carried out using a nano-indenter in order to microscopically investigate the effect of fumed silica on the tribological properties of acrylic based polyurethane coatings. Meanwhile, the bulk and surface morphologies of polyurethane coats embedded with fumed silica were characterized by transmission electron microscope (TEM) and scanning probe microscope (SPM).

## 2. Experimental

### 2.1. Materials

Two fumed silica (one hydrophobic and one hydrophilic) particles were used here. Their properties and manufacturers were presented in Table I. Acrylic resin with a hydroxyl-value of 140 mgKOH/g was prepared in our lab, as shown in the reference [14]. It was offered in 70% acrylic resin solution in butyl acetate. Catalyst of dibutyltin dilaurate (98%) and cross-linking agents of 1,6-hexamethylene diisocyanate homopolymer (HDI, Desmodur N 3300) were obtained from Bayer Company and used as received.

### 2.2. Preparation of acrylic based polyurethane/fumed silica composite coats

Fumed silica particles were directly embedded into acrylic resin solution at 60°C under vigorous stirring for about an hour. The acrylic resin was mixed with HDI without any further dilution based on 1:1.1 mol ratio of —OH/-NCO at room temperature. Just before casting, dibutyltin dilaurate of 0.05 wt% based on the total weight of the resin and polyisocyanate on total solids was mixed thoroughly into the solution. Polyurethane

coats with different thickness were prepared by casting the above solution on Sn-coated Ferrous panels using a drawdown rod and dried at 120°C for 30 min.

## 2.3. Characterization of acrylic based polyurethane/fumed silica composite coatings

### 2.3.1. The morphology

Transmission electron micrographs of the composite coats were obtained by a Hitachi H-600 apparatus (Hitachi Corporation, Japan). Samples were prepared by ultramicrotomy at room temperature, giving sections of about 100 nm in thickness. No further staining was used for contrast improvement. Surface morphology of the samples was examined using a scanning probe microscope (SPM) (NanoScope IIIa, Digital Instruments). The root-mean-square surface roughness (RMS) of the polyurethane coats on Sn-coated Ferrous panels was measured on an area of 100  $\mu\text{m} \times 100 \mu\text{m}$ .

### 2.3.2. Indentation and scratching tests

Micro indentation and scratching tests were carried out with a nano-indenter (Nano Indenter XP, MTS). A Berkovich (3 faced-pyramid) diamond tip was used to indent the surfaces of the samples, and a 90° conical-shaped diamond tip with a radius of 1  $\mu\text{m}$  at its apex was used to scratch the surfaces of samples under either an increasing load or a constant load. Maximum load in the indentation test and maximum load in scratching test were varied from 500  $\mu\text{N}$  to 100 mN. After scratching, the damaged surfaces were examined with SPM, and the micro mar resistances (MMR) under different loads were calculated.

The micro indentation hardness (MIH) of the samples was calculated by dividing the normal force by the contact area of the tip and the sample during indentation. The MMR was defined as the normal force applied during the scratching divided by the cross-section area of the trough after scratching. The Young's modulus was calculated from the slope of the unloading part of the Load ( $P$ )-Penetration ( $h$ ) curves at the turning point. The details of the experiment methods and calculations of hardness and Young's modulus measurements have been described in the reference [15].

## 3. Results and discussion

### 3.1. Morphology of acrylic based polyurethane/fumed silica composites coats

Fig. 1 demonstrates the morphology of acrylic based polyurethane coatings containing 2.5% fumed silica particles. It shows that the hydrophilic silica have a comparable dispersion to the hydrophobic silica probably because the high —OH group content of acrylic resin has great interaction with nano-silica particles. There exist some agglomerates and aggregates in the polyurethane films although some particles reach the nanoscale size (<100 nm). Similar phenomena are observed in the polyurethane films containing 5.0% fumed silica particles, as indicated in Fig. 2.

TABLE I Some properties of fumed silica powders and their suppliers

Types of fumed silica	Aerosil R972	Wacker N-20
Primary particle size (nm)	16	—
Specific surface area ( $\text{m}^2/\text{g}$ ) (BET method)	110 $\pm$ 20	200 $\pm$ 30
Surface properties	—CH <sub>3</sub> , hydrophobic	—OH, hydrophilic
Density (g/l)	90	110
Manufacturer	Degussa Corporation, German	Wacker Company, German

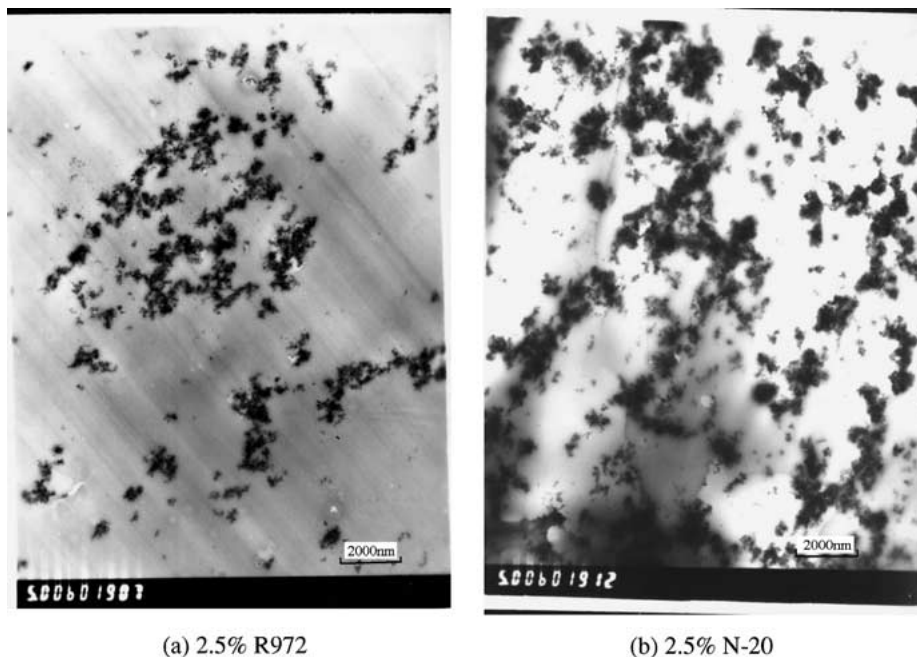


Figure 1 TEM pictures of acrylic based polyurethane coatings containing 2.5% fumed silica particles.

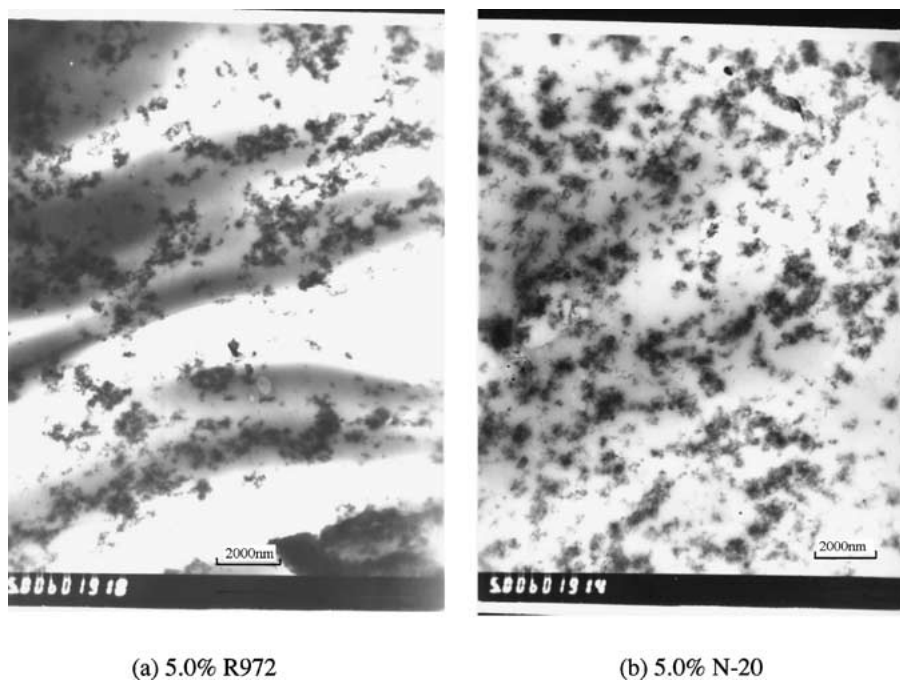


Figure 2 TEM pictures of polyurethane coatings containing 5.0% fumed silica particles.

The surface topographic images of polyurethane coats embedded with different R972 and N-20 content were characterized by SPM and are shown in Figs 3 and 4, respectively. The surface of pure polyurethane films is very smooth (see Fig. 3a). However, after fumed silica are embedded, the surface of polyurethane coats become rougher and rougher with the increasing silica content. The bulges observed on the surface may be due to the aggregates of fumed silica, and the higher the fumed silica content is, the larger the bulges are for the polyurethane containing R972 or N-20 except for the sample containing 5.0% R972, which has poor leveling property of the coating. The root-mean-square surface roughness (RMS) of the polyurethane films

without/with fumed silica in an area of  $100 \mu\text{m} \times 100 \mu\text{m}$  is listed in Table II. It can be clearly seen that the surface roughness increases with increasing fumed silica content. The surfaces of polyurethane

TABLE II The surface roughness of polyurethane coats containing different types of fumed silica particles

Concentration <sup>a</sup> (wt%)	0	2.5	5	7.5	10
RMS	12.9				
R972		50.8	77.3	101	–
N-20		19.8	28.6	88.8	162

<sup>a</sup>Based on the weight of high solid acrylic resin solution with high solid content of 70%.

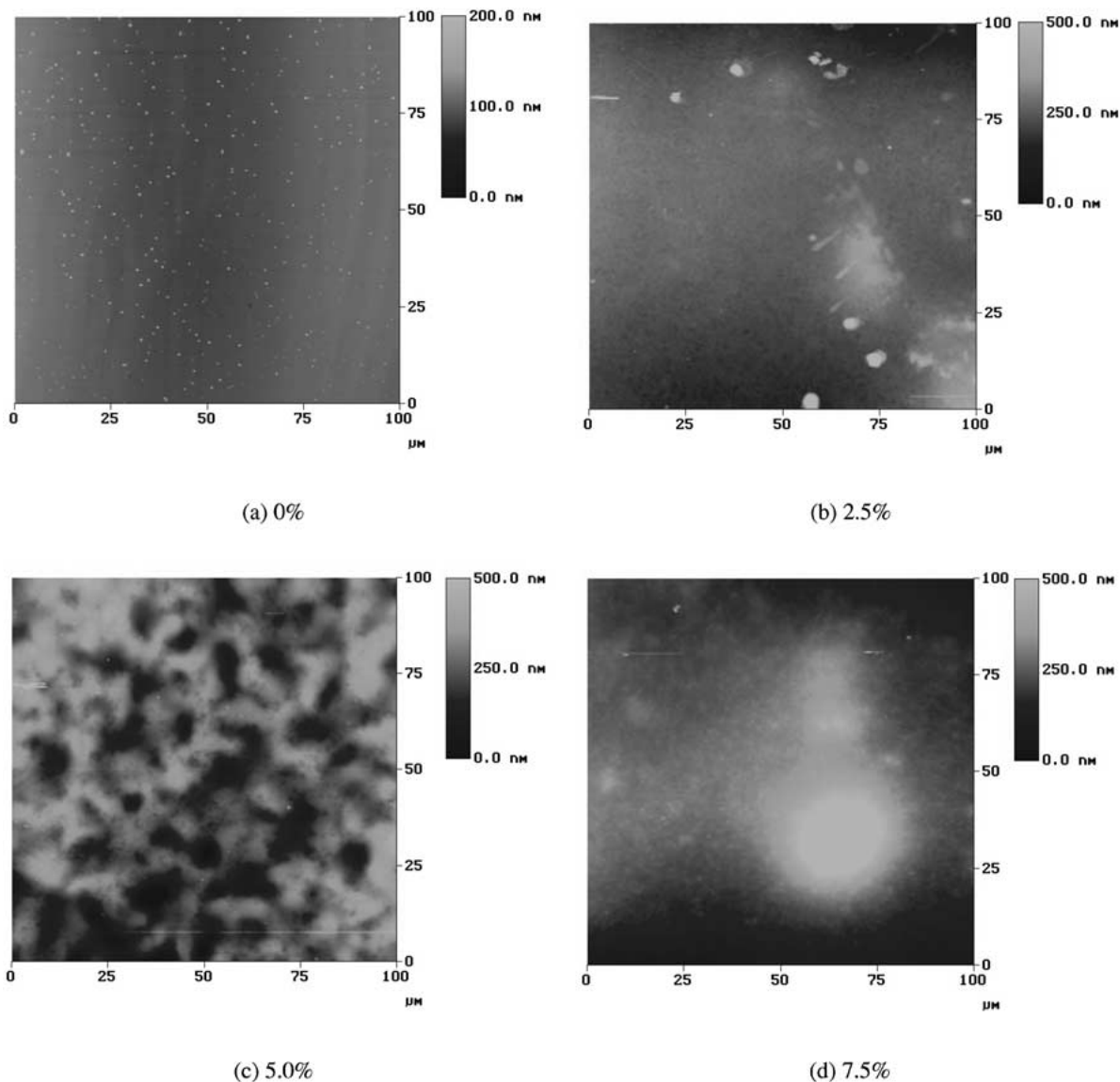


Figure 3 Surface topographic images of polyurethane coats embedded with different R972 content characterized by SPM.

coats containing N-20 are smoother than those containing R972 at the same silica content.

### 3.2. Indentation tests

MIH of the coatings with different concentration of R972 and N-20 under different normal loads are illustrated in Figs 5 and 6, respectively. The data points used in the plot are the average value of more than three individual measurements at different spots at the surface. For the pure polyurethane coats, its MIH decreases with the increment of normal loads. However, for the series of polyurethane coats containing R972, the MIH decreases as normal loads increases under loads less than 20 mN. When the load exceeds 20 mN, the hardness begins to increase. It may not be attributable to the effect of substrate, since the penetration depth (about 2.5–2.6  $\mu\text{m}$  under 20 mN load) is less than 5% of the coating thickness with more than 60  $\mu\text{m}$ . The reason is not clear yet, the relative investigation is underway. For the series of polyurethane coats containing N-20, the MIH keeps decreasing with increasing load in the experimental load range. The higher MIH at lower normal

loads may be resulted from the thin crust of coatings at their surface that is much harder than the bulk [16]. From Figs 5 and 6, it can be concluded that fumed silica can obviously increase the MIH of polyurethane for both R972 and N-20. The absolute values of MIH of polyurethane series with R972 are nearly close to those with N-20.

Figs 7 and 8 show the elastic modulus of the polyurethane coatings as a function of different concentration of R972 and N-20, respectively. It can be seen that fumed silica can improve the elastic modulus of polyurethane coats, and the elastic modulus of polyurethane coats increases as fumed silica content increases. The high elastic modulus is possibly due to the great interaction between fumed silica particles and organic matrix since fumed silica has the large specific surface area, which have been confirmed in our previous study on the effect of nano-SiO<sub>2</sub> and micro-SiO<sub>2</sub> particles on Young's modulus of polyurethane [14].

Except for the pure polyurethane coats, the elastic modulus of all the polyurethane coats embedded with fumed silica keep constant with increasing normal

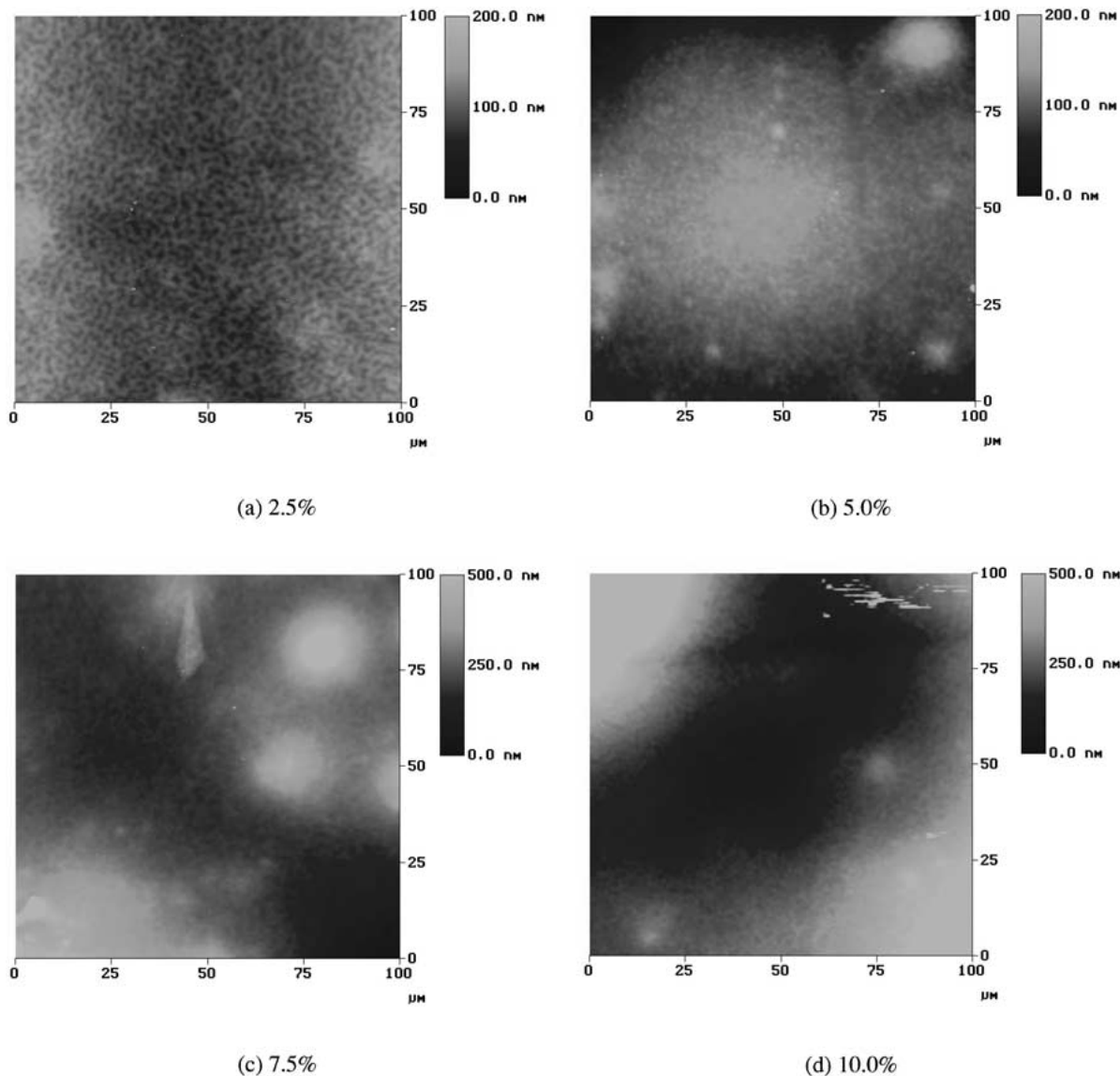


Figure 4 Surface topographic images of polyurethane coats embedded with different N-20 content characterized by SPM.

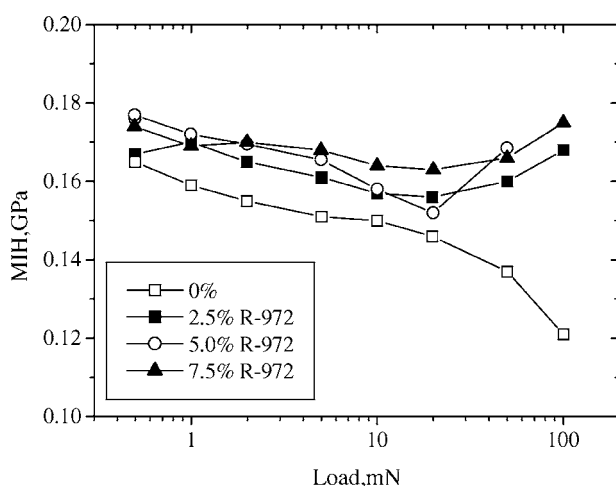


Figure 5 The change of MIH of the films with different R972 content.

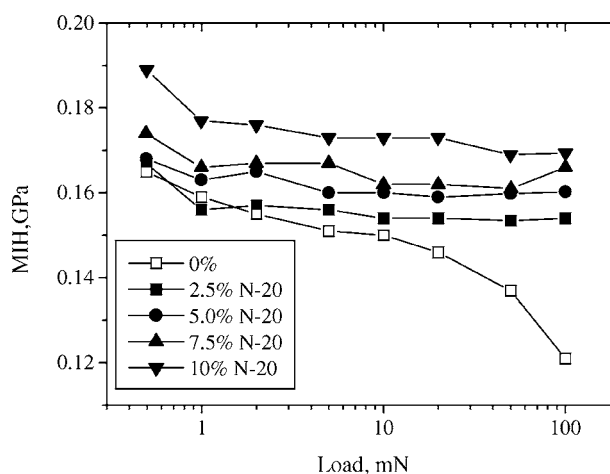


Figure 6 The change of MIH of the films with different N-20 content.

loads under loads about less than 20 mN, but increase when loads exceed 20 mN, just as observed in MIH of polyurethane series with R972. It seems that the load of 20 mN is the turn point for the changes of mechanical properties of the polyurethane containing R972. This

is probably because there exists a concentration gradient in the polyurethane/fumed silica composite films. The fumed silica particles prefer to settle in the bulk not move towards polymer surface, just as characterized by XPS in our another paper [14].

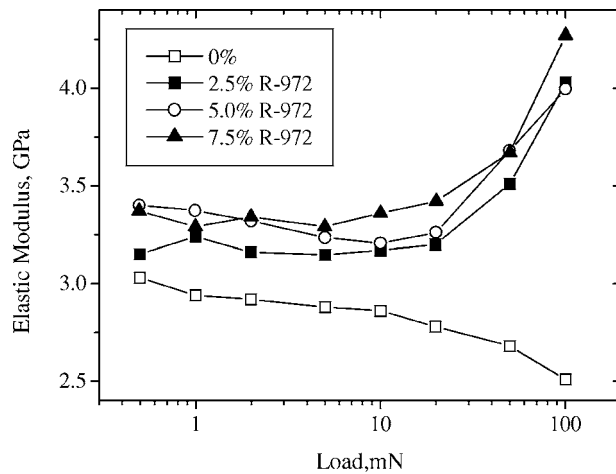


Figure 7 The elastic modulus of polyurethane films containing different R972 contents.

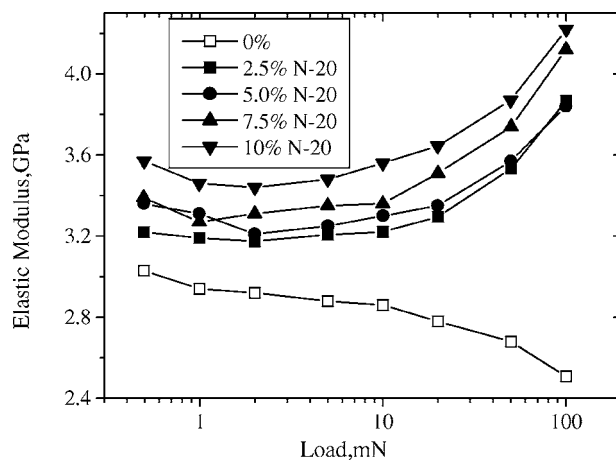


Figure 8 The elastic modulus of polyurethane films containing different N-20 contents.

### 3.3. Scratching tests

Scratching with an increasing load was used to determine the critical force for cracking. A typical crack pattern for the polyurethane coats with 2.5% R972 is presented in Fig. 9. It can be seen that the crack of the sample is limited between the two shoulders. Other polyurethane/fumed silica composite coats have

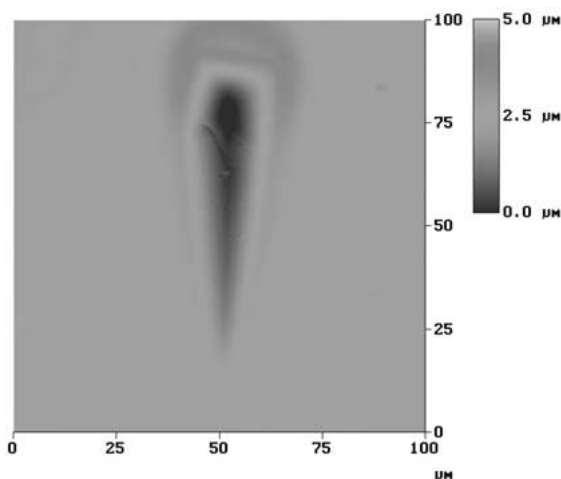


Figure 9 A typical topographic image for the polyurethane coats with 2.5% R972 after scratching.

TABLE III Critical force and corresponding penetration depth for polyurethane/fumed silica composite coats

Type of fumed silica	Content of fumed silica <sup>a</sup>	Critical force (mN)	Penetration depth ( $\mu\text{m}$ )
R972	2.5%	$51 \pm 1$	11.5
	5.0%	$58 \pm 3$	9.5
	7.5%	$60 \pm 4$	8.0
N-20	2.5%	$50.9 \pm 0.4$	8.8
	5.0%	$50.4 \pm 1$	8.5
	7.5%	$52 \pm 3$	7.3
	10.0%	$54 \pm 2$	7.6

<sup>a</sup>Based on the weight of high solid acrylic resin solution with 70% solid content.

the same crack pattern as shown in Fig. 9, but the critical normal forces for cracks are somewhat different. The critical force for cracking of each sample and the corresponding penetration depth are listed in Table III. It can be seen that critical force slightly increases and penetration depth slightly decreases for polyurethane coats containing R972 or N-20, indicating fumed silica can enhance the strength of polyurethane coats. Table III also shows that at the same fumed silica content, polyurethane coats with R972 have relatively higher critical force and penetration depth than that with N-20. Thus, polyurethane/R972 composite coats are much tougher than polyurethane/N-20 composite coats. This may be due to more crosslinking reactions between isocyanate group and hydroxyl group on the surface of N-20 particles than between isocyanate group and hydroxyl group on the surface of R972 particles during curing since the former has more  $-\text{OH}$  groups than the latter.

Scratching with a constant normal load was also carried out for all polyurethane coats with/without fumed silica. The percentages of elastic response, plastic deformation and fracture was calculated according to the method described by Jones *et al.* [16] and shown in Figs 10 and 11 for the polyurethane coats with R972 and N-20, respectively. For most cases of the scratching, elastic response, plastic deformation and fracture are all observed, but in our experimental range of normal force, the percentage of fracture is small comparing with the percentages of elastic response and plastic deformation. As normal force increases, the percentage of elastic response drops and the percentage of plastic deformation rises not only for polyurethane/R972 composite coats but also for polyurethane/N-20 composite coats. For all the polyurethane/fumed silica composite coats, the percentage of elastic response nearly equals the percentage of plastic deformation under normal force of 5 mN and become only half of the percentage of plastic deformation under normal force higher than 20 mN. But the content of fumed silica has no obvious impact on the response of marring stress and the both hydrophobic and hydrophilic fumed silica have almost the same influence. However, for the pure polyurethane coats, the percentage of elastic response is close to the percentage of plastic deformation and both of them keep nearly unchanged with increasing normal force. Therefore, fumed silica can increase the plasticity of acrylic based polyurethane coats.

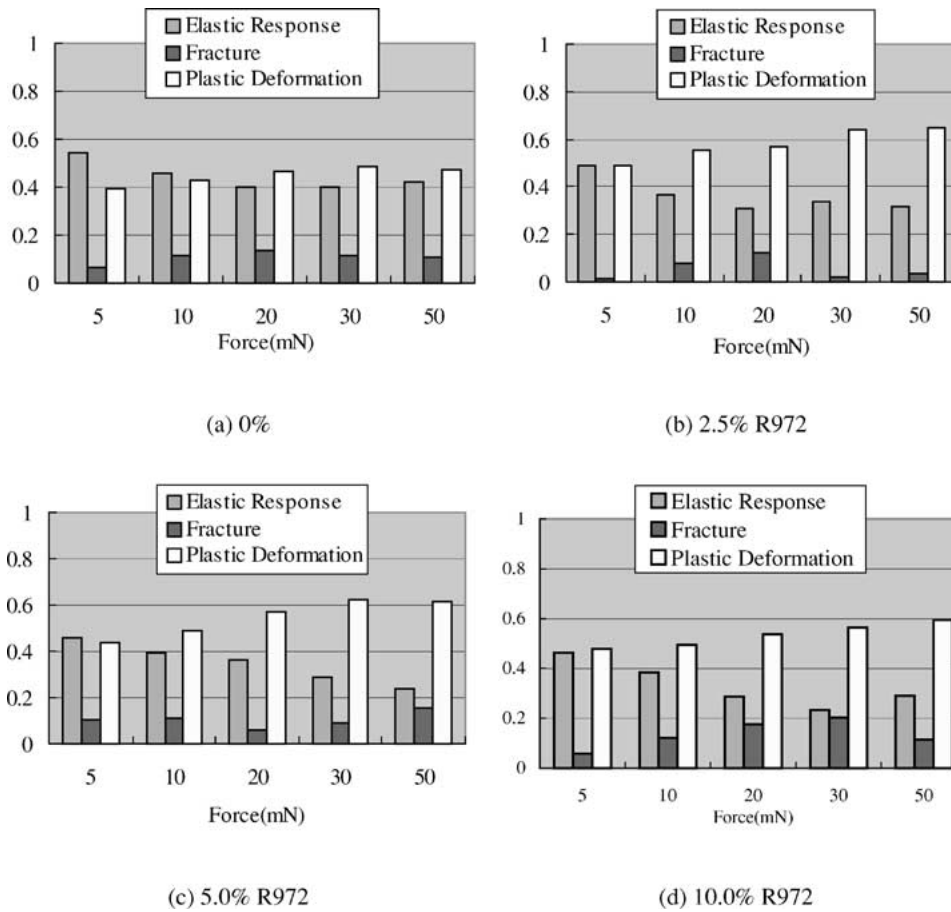


Figure 10 The percentage of elastic response, plastic deformation and fracture of the polyurethane/R972 composite coats after scratching under constant normal force.

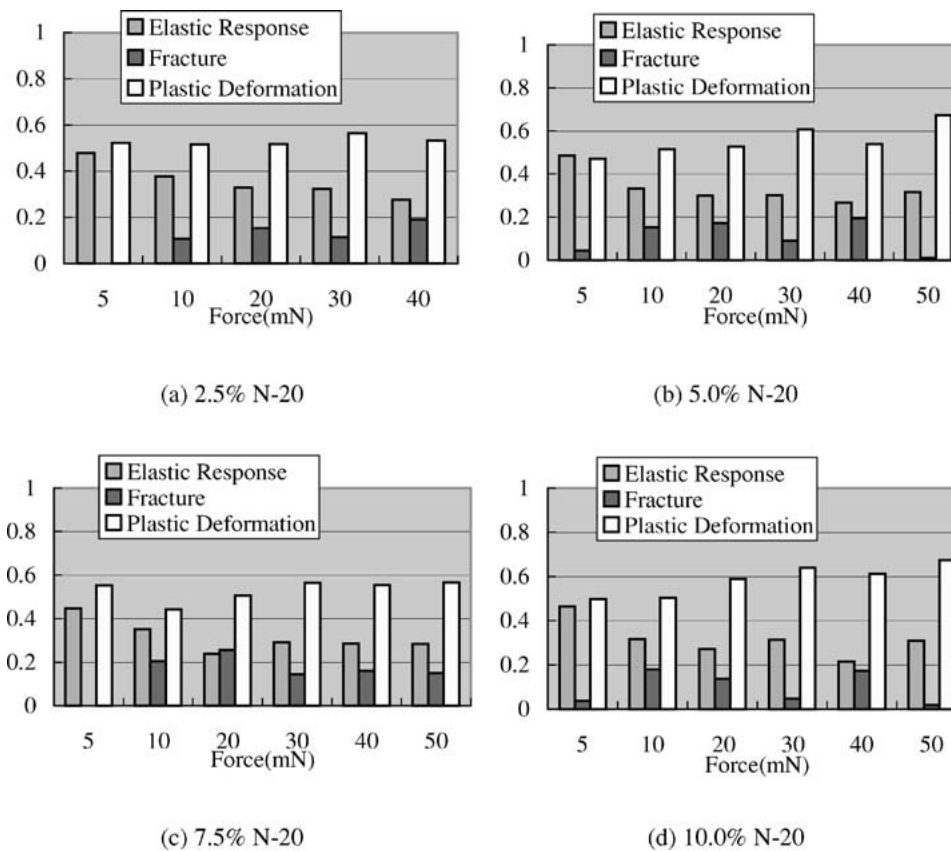


Figure 11 The percentage of elastic response, plastic deformation and fracture of the polyurethane/N-20 composite coats after scratching under constant normal force.

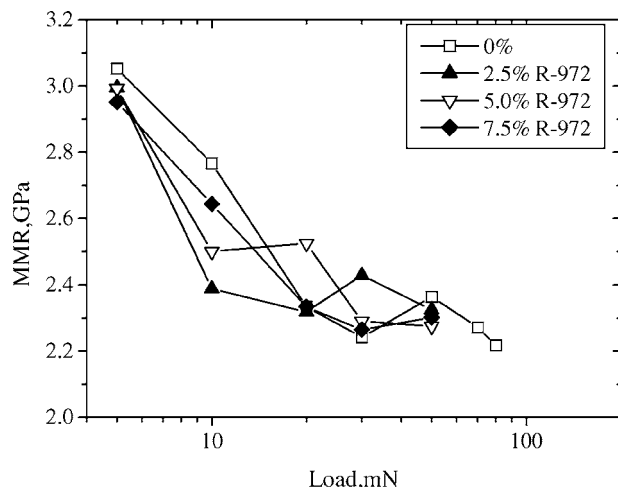


Figure 12 MMR of polyurethane films with different R972 contents.

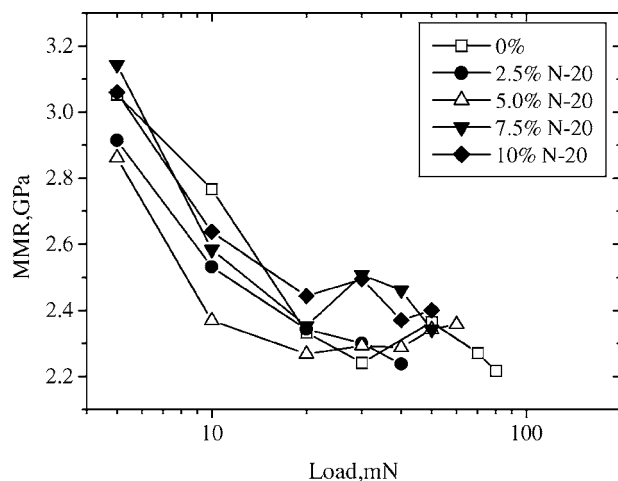


Figure 13 MMR of polyurethane films with different N-20 contents.

The MMR of polyurethane coats with different R972 and N-20 contents are plotted in Figs 12 and 13, respectively. For all polyurethane coats, the values of MMR quickly decrease with increasing normal force under lower normal force and level off under normal force larger than 20 mN. The turn point of 20 mN is similar to that observed in the change of elastic modulus above. However, since the factors influencing on MMR are more complicated, the changes of MMR with either R972 or N-20 content increasing are irregular at a certain normal load. But one point is clear, that is, both R972 and N-20 has no improvement in MMR of polyurethane coats, which is different from what was found in acrylic based polyurethane embedded with nano-silica obtained from chemical method [14].

#### 4. Conclusions

(i) Fumed silica particles cause rough surfaces of polyurethane films, and polyurethane surfaces become rougher and rougher with the increasing silica content.

(ii) In our experimental range, the normal load obviously influences the MIH, elastic modulus, response to marring stress and MMR. A turn point of 20 mN normal force is observed in the change of tribological

properties (such as MIH, elastic modulus and MMR of polyurethane/R972 composite coats and elastic modulus and MMR of polyurethane/N-20 composite coats) with increasing loads.

(iii) The MIH and critical force for crack can be improved by addition of both hydrophobic and hydrophilic fumed silica, and increase as the content of fumed silica increases. Scratching tests show that the polyurethane/fumed silica composite coats are higher plastic than pure polyurethane coats. But the content of fumed silica has no obvious impact on the response to marring stress and MMR of polyurethane/fumed silica composite coats. Additionally, both hydrophobic and hydrophilic fumed silica have very close influence on the tribological properties of acrylic based polyurethane coatings.

#### Acknowledgments

We would like to thank the National '863' Foundation, Shanghai Nano Special Foundation, the Key Project of China Educational Ministry, the Doctoral Foundation of University, Trans-century Outstanding Talented Person Foundation of China Educational Ministry, and Shanghai Shuguang Foundation for financial support for this research.

#### References

1. A. M. TORRÓ-PALAU, J. C. FERNÁNDEZ-GARCÍA, A. C. ORGILÉS-BARCELÓ, T. P. FERRÁNDIZ-GÓMEZ and J. M. MARTÍN-MARTÍNEZ, *Macromol. Symp.* **169**(1) (2001) 191.
2. H. BARTHEL, M. DREYER, T. GOTTSCHALK-GAUDIG, V. LITVINOV and E. NIKITINA, *ibid.* **187**(1) (2002) 573.
3. H. SHIRONO, Y. AMANO, M. KAWAGUCHI and T. KATO, *J. Coll. Interf. Sci.* **239**(2) (2001) 555.
4. M. ETTLINGER, T. LADWIG and A. WEISE, *Prog. Org. Coat.* **40** (2000) 31.
5. L. GABRIELE, L. THORSTEN, V. VLASTA, F. STEPHANIE and M. JÜRGEN, *ibid.* **45**(2/3) (2002) 139.
6. B. ABRAMOFF and J. COVINO, *J. Appl. Polym. Sci.* **46**(10) (1992) 1785.
7. Y. C. OU, F. YANG, Y. ZHUANG and Z. N. QI, *Acta Polym. Sini.* **2** (1997) 199 (in Chinese).
8. B. MANFRED, E. THEODOR, G. STEFAN, K. BERND, Y. PHILIP, J. GERHARD and D. ULRIKE, United States Patent, US 6020419 (2000).
9. Y. HARA, T. MORI and T. FUJITANI, *Prog. Org. Coat.* **40** (2000) 39.
10. W. D. SHEN, B. JIANG, S. M. GASWORTH and H. MUKAMAL, *Tribol. Intern.* **34** (2001) 135.
11. L. LIN, G. S. BLACKMAN and R. R. MATHESON, *Prog. Org. Coat.* **40** (2000) 85.
12. P. BERTRAND-LAMBOTTE, J. L. LOUBET, C. VERPY and S. PAVAN, *Thin Solid Films* **398** (2001) 306.
13. B. BHUSHAN, *Wear* **251** (2001) 1105.
14. S. X. ZHOU, L. M. WU, J. SUN and W. D. SHEN, *Prog. Org. Coat.* **45** (2002) 33.
15. W. C. OLIVER AND G. M. PHARR, *J. Mater. Res.* **7** (1992) 1564.
16. F. N. JONES, W. D. SHEN, S. M. SMITH, Z. H. HUANG and R. A. RYNTZ, *Prog. Org. Coat.* **34** (1998) 119.

Received 15 May  
and accepted 5 August 2003